Journal of Ceramic Processing Research. Vol. 23, No. 3, pp. 350~355 (2022)
(Received 1 January 2022, Received in revised form 6 February 2022, Accepted 9 February 2022)
https://doi.org/10.36410/jcpr.2022.23.3.350

J O U R N A L O F
Ceramic Processing Research

Optical properties of the Bi_2O_3 - B_2O_3 - ZnO glass system combined with TiO_2 or Ag/TiO_2

Kieu Do Trung Kien[a,b,*], Nguyen Vu Uyen Nhi[a,b], Huynh Ngoc Minh[a,b] and Do Quang Minh[a,b,*]
[a]*Department of Silicate Materials, Faculty of Materials Technology, Ho Chi Minh City University of Technology (HCMUT), 268 Ly Thuong Kiet street, District 10, Ho Chi Minh City, VietNam*
[b]*Vietnam National University Ho Chi Minh City, Linh Trung Ward, Thu Duc District, Ho Chi Minh City, Vietnam*

Lead-free Bi_2O_3 - B_2O_3 - ZnO glass is a commonly synthesized glass system at low temperatures for coating applications for materials such as ceramic, glass, metal, etc. TiO_2 or Ag/TiO_2 composite are usually photocatalyst for antimicrobial application. In this study, TiO_2 or Ag/TiO_2 were combined with the Bi_2O_3 - B_2O_3 - ZnO glass system by the technique of rapid cooling of molten glass at 1200°C. The influence of the TiO_2 or Ag/TiO_2 on the optical characteristics of the Bi_2O_3 - B_2O_3 - ZnO glass system was performed by using X-ray diffraction, Fourier Transform Infrared Spectroscopy, and Ultraviolet-Visible Spectroscopy techniques. The analytical results showed that the band gap energy of the Bi_2O_3 - B_2O_3 - ZnO glass system had a low value. The band gap energy of the system increased with the addition of TiO_2 and decreased slightly with the addition of Ag/TiO_2. In addition, when Ti_2O or Ag/TiO_2 were added, the glass system appeared crystals such as anatase, rutile and silver oxide on an amorphous background. These crystals cause the system's transmittance to decrease and reflectance to increase. However, the appearance of these crystals promises that Bi_2O_3 - B_2O_3 - ZnO glass materials can be applied as antibacterial materials. The antibacterial property is due to the photocatalytic effect of TiO_2 and the ability to kill bacteria Ag_2O.

Keywords: Bi_2O_3 - B_2O_3 - ZnO, Ag/TiO_2, photocatalyst, antimicrobial application.

Introduction

The Bi_2O_3 - B_2O_3 - ZnO glass system (BBZ) is a kind of glass synthesized at low temperatures [1, 2]. In the structure network of the BBZ, the $[BO_n]^{(2n-3)-}$ may create coordinated polyhedral and takes on the task of creating the glass network oxide. The $[BiO_3]^{3-}$ units and $[BiO_6]^{9-}$ octahedral can also play a role in the formation of the glass lattice. ZnO plays a role in increasing the glass's stability and making the glass system easy to shape. BBZ has been researched and applied as a shielding material for gamma, transparent dielectric layer, photonic applications, etc [3-5]. Because the low glass forming temperature is one of the important properties of the BBZ, its common application is a coating on different surfaces [6]. To diversify the applicability, some studies have added other elements to the BBZ to improve its properties.

TiO_2 is known as a material with a photocatalytic effect and biologically benign. Therefore, TiO_2 is often applied to treat toxic substances that cause pollution in the environment [7]. TiO_2 exists in different polymorphs such as rutile, anatase, brookite, etc. The band gap (E_g) of TiO_2 is large (~3.0 eV of rutile and ~3.2 eV of anatase) [8]. Therefore, the addition of TiO_2 to the glass not only improves chemical stability [9] but also increases the photocatalytic ability of its. However, one lack of TiO_2 is that photochemistry is difficult to activate with visible light hinders its application. D. Ning et al. showed that doped some precious metals could improve the photocatalytic ability and antibacterial effect [10]. Transition metals, precious metals are usually doped in TiO_2 crystal lattice and combined with semiconductor materials with narrow band gap can create materials more sensitive to visible light, increase their photocatalytic efficiency. Among these metals, silver is cheaper and can be used as a visible sensitive material for photocatalytic activity [11]. Silver nano-particles on semiconductors providing better electron transport would effectively improve photocatalytic activity [12]. In addition, due to its antibacterial properties and low toxicity, metallic silver and oxide silver have long been considered effective antibacterial agents [13]. Therefore, silver doping with TiO_2 promises to increase the antibacterial ability of TiO_2. Besides, doping silver with TiO_2 also makes silver chemically stable and releases silver ions more slowly.

As mentioned above, the BBZ is a low-temperature glass system that can be applied as coatings for ceramic, glass, and metal. When doped with TiO_2 and silver into the glass base can also control the energy of the band gap, making glass more sensitive to visible light, increasing the photocatalytic efficiency and antibacterial

*Corresponding author:
Tel : +(84.8) 8 661 320
Fax: +(84.8) 8 661 843
E-mail: kieudotrungkien@hcmut.edu.vn (Kieu Do Trung Kien),
mnh_doquang@hcmut.edu.vn (Do Quang Minh)

properties. In this study, the optical properties of the BBZ were investigated when combined with TiO_2 and Ag/TiO_2. The change in optical properties of the BBZ was studied by using X-ray diffraction, Fourier Transform Infrared Spectroscopy, and Ultraviolet-Visible Spectroscopy methods.

Materials and Methods

The chemical composition of the BBZ was chosen by considering the equilibrium phase diagram of the ternary system of the BBZ [14]. The selected basic chemical compositions were (% wt.): 73.8% Bi_2O_3, 15.3% B_2O_3, and 10.9% ZnO. TiO_2 and Ag/TiO_2 were added into the basic glass compositions according to the ratios given in Table 1. The raw materials used in this study are also presented in Table 1. The samples were fabricated as shown in Fig. 1. The raw materials were mixed. The mixtures were formed into glass by using conventional melt quenching techniques. The muffle furnaces (L5/13/P330 Nabertherm model) was used to melt each batch of this glassware in a Pt crucible at 1,200 °C for 90 minutes. The heating rate was 5°C/min. Glasses after vitrifying were milled in a planetary mill for 2 hours to obtain a fine glass powder with sizes passed through a sieve with 125 μm.

Table 1. The raw materials and chemical compositions of glass samples

Raw materials	Supply Oxide	Samples (%w.t)				
		T_0A_0	T_5A_0	T_5A_1	$T_{10}A_0$	$T_{10}A_1$
$Bi_5O(OH)_9(NO_3)_4$	Bi_2O_3	73.8	73.8	73.8	73.8	73.8
H_3BO_3	B_2O_3	15.3	15.3	15.3	15.3	15.3
ZnO	ZnO	10.9	10.9	10.9	10.9	10.9
TiO_2	$TiO_2^{(*)}$	0	5	5	10	10
$AgNO_3$	$Ag^{(*)}$	0	0	1	0	1

(*) According to 100% by weight of base glass.

The optical properties of the glasses were measured by UV-Vis reflectance spectroscopy. The model was used Lambda 950 of Perkin Elmer. The UV-Vis analysis condition was wave range from 250-880 nm, the step of 5 nm. The thickness of the samples was 1 cm. From the UV-Vis results, it is possible to calculate the band gap energy of the formed glass by formula (1). The relationship between band gap energy and absorption coefficient α is shown in formula (1) [15]. Where α is molar absorptivity, *h* is Planck's constant, υ is the frequency of light (υ = c/λ), c is the speed of light, λ is the wavelength of light, B is constant, E_g is band gap energy. According to previous study, the optical properties of the BBZ exhibit an indirect band gap. Therefore, the value of m is chosen to be 1/2 for the BBZ [16].

$$(\alpha h\upsilon)^m = B(h\upsilon - E_g) \quad (1)$$

To determine the band gap energy, the graph and functional eq. (2) are determined from the results of UV-Vis spectroscopy.

$$(\alpha h\upsilon)^m = f(E) \quad (2)$$

The E value of the function (2) is determined from UV-Vis results according to formula (3). The value of absorption coefficient α of function (2) is determined from UV-Vis results and Beer – Lambert's equation according to formula (4). Where A is the absorbance and is determined on the UV-Vis spectrum, l cm is the thickness of the sample.

$$E = hc/\lambda \quad (3)$$

$$\alpha = 2.303A/l \quad (4)$$

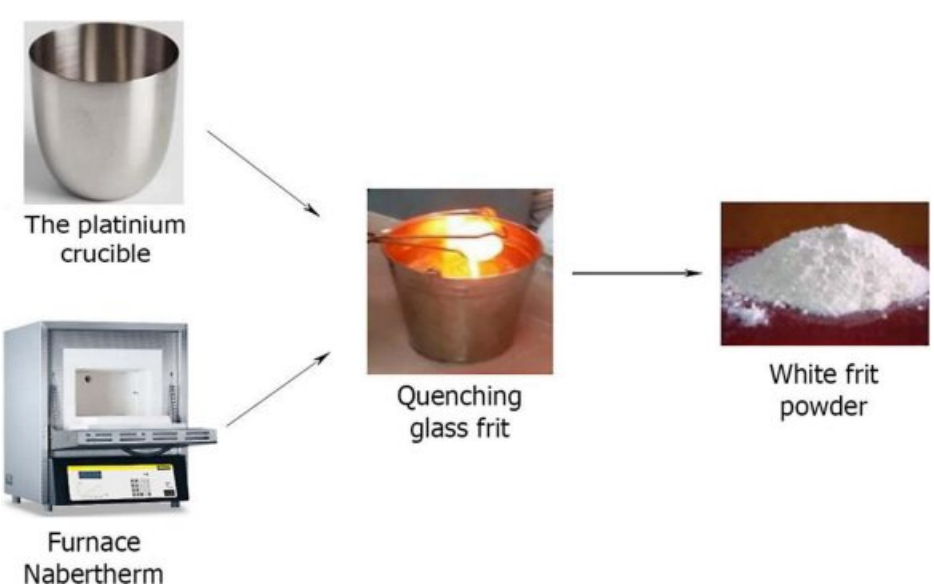

Fig. 1. A diagram of the prototyping process.

The inflexion point of graph (2) is determined by solving the second derivative eq. (5). Then, construct a tangent equation to the function $(\alpha h\upsilon)^m = f(E)$ at the inflexion point. The intersection between the tangent equation and the X-axis is the value E_g.

$$f''(E) = 0 \quad (5)$$

The microstructure characteristics of these glasses were analyzed by using X-ray diffraction (XRD) methods, Fourier Transform Infrared Spectroscopy (FTIR). The XRD analyzer was a D2 Phaser model of Bruker. The XRD analysis condition was scanning 2theta degree from 20-80°, scanning step of 0.02°, and use Cu K_α radiation (λ = 0.154 nm). The FTIR analyzer was the Nicolet 6700 model of Thermo Scientific. The FTIR analysis condition was scanning wavenumber from 450-2000 cm^{-1} and scanning step of 0.96 cm^{-1}.

Results and Discussions

Fig. 2. shows transmittance spectrum of glass samples after vitrifying at 1,200 °C for 90 min. The results of the transmittance spectrum in Fig. 2. showed that the background glass (sample T_0A_0) had the highest transmittance. This property demonstrated the optical transparency of the BBZ. However, with the addition of TiO_2 to the base glass (T_5A_0 and $T_{10}A_0$), the transmittance of the glass system decreased. The transmittance of the system continued to decrease with increasing TiO_2 content from 5% to 10%. When Ag/TiO_2 was added to the base glass system (T_5A_1 and $T_{10}A_1$), the transmittance decreased compared with the sample only adding TiO_2.

Effect of the band gap on the transmittance

V. Anand et al. showed that the transmittance of glass decreases due to the reduction in band gap energy of glass [17]. Fig. 3. and Fig. 4. plot between $(ah\upsilon)^{1/2}$ and

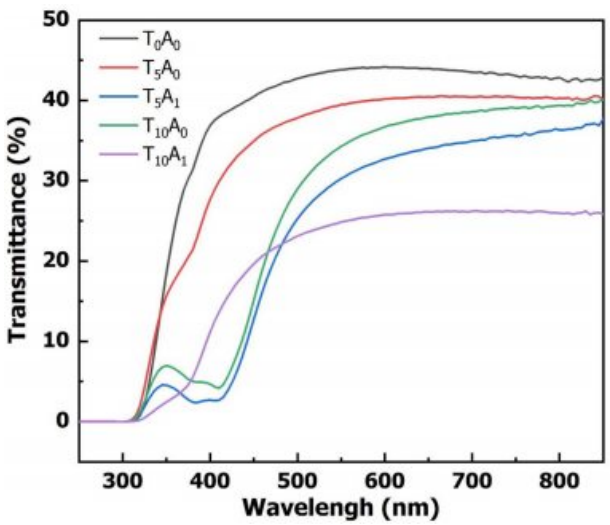

Fig. 2. The transmittance spectrum of glass samples.

energy used to determine the band gap energy of the glass samples from the UV-Vis spectrum. The Dose-Response model has been selected to build the regression equation passing through the points represented on the graph. The intersection between the X-axis and the tangent line at the inflexion point of the regression equation helps determine the glass sample's band gap energy value. The band gap energy results in Fig. 3. and Fig. 4. showed that the band gap energy of the BBZ had a low value (2.098 eV).

When TiO_2 or Ag/TiO_2 was added, the band gap energy of the glass system was increased compared to the base glass system. With the glass samples only adding TiO_2, the band gap energy was increased to 2.478 eV (T_5A_0) and 2.695 eV ($T_{10}A_0$). With the glass samples supplemented with Ag/TiO_2, the band gap energy was slightly reduced to 2.337 eV (T_5A_1) and 2.642 eV ($T_{10}A_1$). This study's band gap energy determination results show that the band gap energy was increased when TiO_2 or Ag/TiO_2 was added to the basic glass. Therefore, it could be seen that, in this case, the change band of gap energy was not the cause of the decrease in optical transmittance of the BBZ glass system.

With the glass samples only adding TiO_2, Fig. 3. showed that the addition of TiO_2 to the BBZ prolonged the band gap energy of the basic glass system. The increased band gap energy with the addition of TiO_2 could open up applications as photocatalysts for these materials. When TiO_2 receives radiation energy, the electron hopping from the valence region to the conduction region will help to form holes (h^+) and electrons (e^-). The hole (h^+) will ionize water molecules to form (•OH) and the electron (e^-) will ionize oxygen to form ($•O^{2-}$) [18]. The reaction between these ions with organic radicals in bacteria will create an antibacterial material.

Fig. 4. also showed that when Ag/TiO_2 was added to the BBZ, the band gap energy decreased slightly compared to the case of adding only TiO_2. The band gap energy of samples supplemented with 5% TiO_2 and 1% Ag was decreased from 2.478 eV to 2.336eV, the band gap energy of samples supplemented with 10% TiO_2 and 1% Ag was decreased from 2.695 eV to 2.642 eV. Silver reduces the band gap by creating traps between the conduction and valence bands. Reducing the band gap energy can reduce the photocatalytic performance of the BBZ. However, the addition of silver to the glass composition promises to improve the bactericidal ability of glass [13]. The band gap energy change explained by the interaction between Ag, TiO_2, and the base glass can be observed by FTIR spectral analysis.

Fig. 5. shows the FT-IR spectrum of the glass samples after vitrifying at 1,200 °C at different compositions. The FTIR spectra of T_0A_0 in Fig. 5. showed that the vibrations such as 1,643 cm^{-1} was typical for the -OH group; 877 cm^{-1} was a characteristic of planar $[BiO_3]^{3-}$;

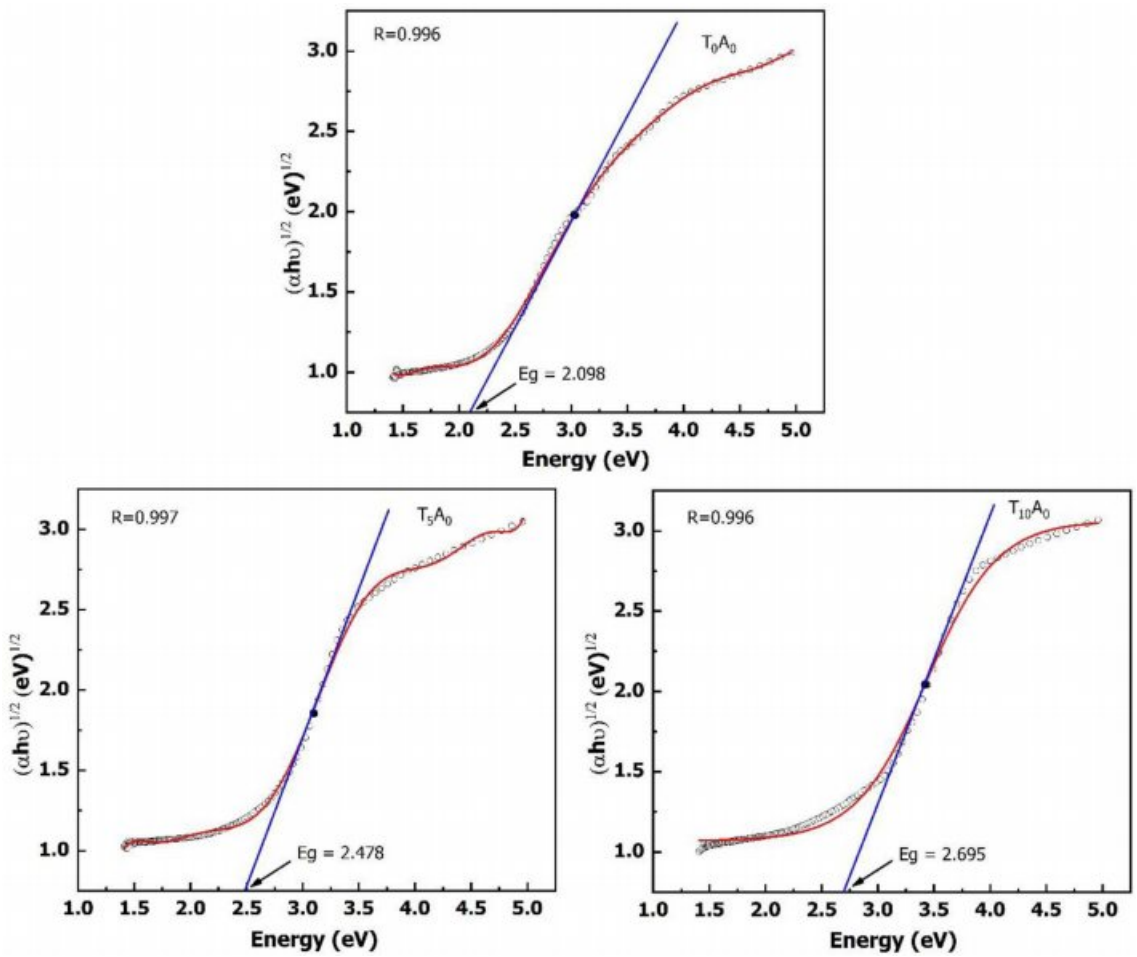

Fig. 3. Eg of the T_0A_0, T_5A_0, and $T_{10}A_0$ samples.

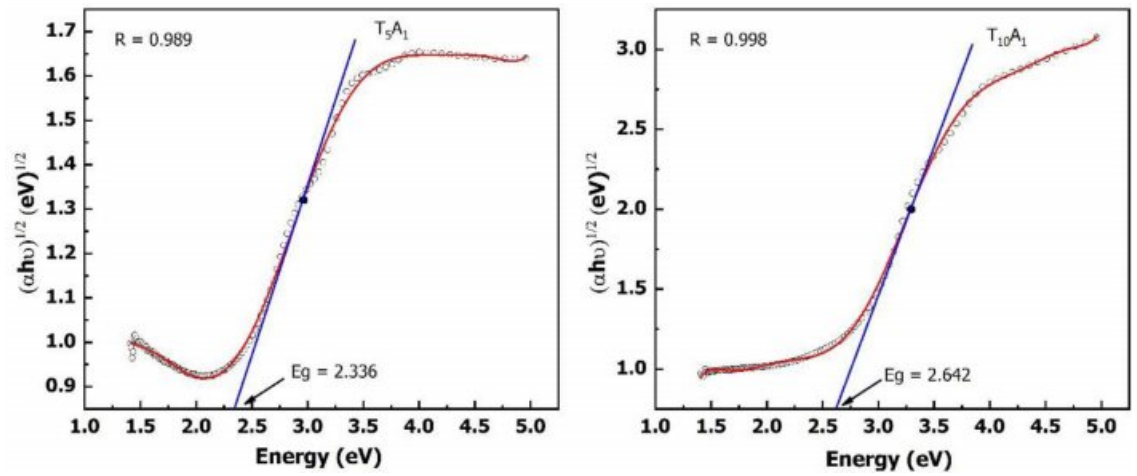

Fig. 4. Eg of the T_5A_1 and $T_{10}A_1$ samples.

715, 620 cm^{-1} represented the tetrahedron $[BiO_6]^{9-}$; 1279, 609 cm^{-1} were typical for planar $[BO_3]^{3-}$; 1144, 607 cm^{-1} were typical for tetrahedral $[BO_4]^{5-}$; 435 cm^{-1} was typical for the ZnO group [19-22]. The $[BO_3]^3$, $[BO_4]^{5-}$, $[BiO_3]^{3-}$, and $[BiO_6]^{9-}$ groups were the basis for forming the glass lattice in the BBZ. Bi_2O_3 and B_2O_3 were also why the BBZ glass system could be formed at low temperatures.

With the glass samples only adding TiO_2, besides the characteristic vibrations of the BBZ, the FTIR spectrum of T_5A_0 and TA_0 also appeared to vibrate at wavenumber position 1,456-1,465 cm^{-1} and 1,057 cm^{-1}. These vibrations

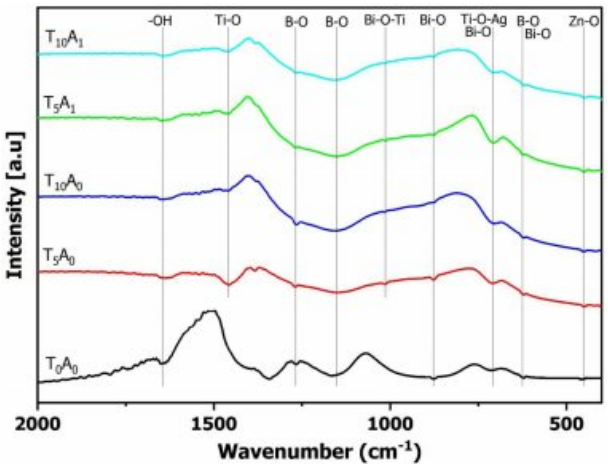

Fig. 5. The FTIR spectrum of the glass samples.

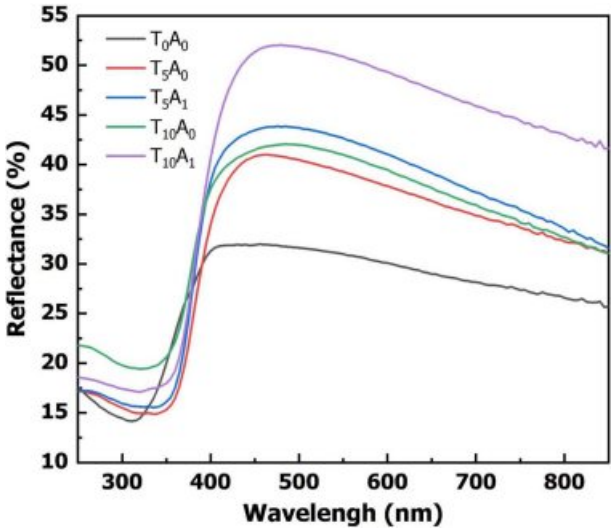

Fig. 6. The reflectance spectrum of glass samples.

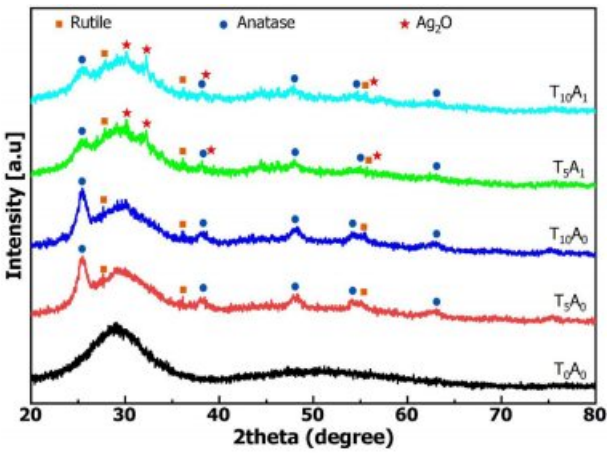

Fig. 7. The XRD patterns of glass samples.

are characteristic of the Ti-O-Ti bond and the Bi-O-Ti bond [19, 23]. The Ti-O-Ti bond demonstrated the presence of TiO_2 distributed in the base glass. As mentioned in Fig. 3., the band gap energy of the BBZ increased when TiO_2 was added to the composition. This result is contrary to most previous studies on the addition of TiO_2 to the base glass [24, 25]. In this study, TiO_2 content was used in a large amount (5-10% compared to 0-2% TiO_2 of previous studies). The vibrations of Bi-O-Ti and Ti-O-Ti simultaneously appeared on the FTIR spectrum, indicating that TiO_2 not only participates in binding with bismuth to form glass but also exists in free form. The free TiO_2 extended the band gap of the BBZ. With the additional samples Ag/TiO_2, the wavenumber at 702-708 cm^{-1} on the FTIR spectrum of T_5A_1 and $T_{10}A_1$ has an absolute intensity higher than other samples. This wavenumber position corresponds to the position of the Ti-O-Ag bond [26]. The Ti-O-Ag bond causes an additive effect to increase the intensity of the vibration at 702-708 cm^{-1}. The interaction between Ag and TiO_2 formed the Ti-O-Ag bond. The formed bond has reduced the band gap energy of the BBZ, as shown in Fig. 3. and Fig. 4.

Effect of the formed crystals on the transmittance

Besides the band gap energy, the transmittance of the glass is also affected by the number of crystals in the base glass. The reflectance analysis results in Fig. 6. showed that the reflectance increased when TiO_2 or Ag/TiO_2 were added to the BBZ. When adding Ag/TiO_2 to the system, the reflectance increased more strongly than adding only TiO_2. This result implied that the crystal could be formed when adding TiO_2 or Ag/TiO_2. To clarify this issue, the XRD analysis method was used to evaluate the phase composition of the glass samples.

Fig. 7. shows the XRD pattern results of the glass samples after vitrifying at 1,200 ºC. The XRD patterns showed that in all samples, a large diffraction area of the amorphous phase has appeared from 20 to 40º [3]. This result demonstrated that there was glass formation in all ingredients at 1,200 ºC vitrifying temperature. The XRD result of T_0A_0 showed no appearance of crystal peaks. The main phase was the amorphous phase. For samples with TiO_2 or Ag/TiO_2, amorphous was still the main phase appearing on the XRD patterns. However, besides the amorphous phase, the XRD patterns of these samples also appeared crystals. The crystals formed include anatase, rutile and Ag_2O. These crystals caused the higher reflectance of the T_5A_0, T_5A_1, $T_{10}A_0$, and $T_{10}A_1$ than the T_0A_0 sample, as mentioned in the results in Fig. 6.

Q. Chen et al. showed that added TiO_2 with a low content would participate in the glass forming process, and the XRD pattern wouldn't appear peak of the TiO_2 crystal [25]. In this study, with 5% and 10% TiO_2 used, the XRD pattern of glass samples containing TiO_2 (in Fig. 7.) appeared diffraction peaks representing anatase (R060277) at diffraction positions 25.22º, 38.43º, 47.85º, 53.72º, and 62.63º [27] and rutile (R060745) at the diffraction position 27.34º, 36.20º, and 54.86º [28]. The

formed anatase and rutile crystals proved that TiO_2 not only participated in glass formation but also formed free crystals distributed on an amorphous background. Anatase and rutile are two minerals with high band gap energy. Therefore, anatase and rutile created an additive effect to increase the band gap of the BBZ. Anatase and rutile are also photocatalytic minerals. The presence of these two minerals will also open the possibility of photocatalysis for glass. The BBZ with a large amount of TiO_2 added can be applied as a bactericidal glass.

For samples using silver (T_5A_1 and $T_{10}A_1$), the XRD patterns in Fig. 7 showed the presence of Ag_2O. Ag_2O (JCPDS 41-1104) was shown at the diffraction positions of 26.7°, 32.8°, 38.1°, and 54.9° in Fig. 7 [29]. As analyzed, the FTIR spectrum (Fig. 5) of T_5A_1 and $T_{10}A_1$ appeared vibration corresponding to the Ti-O-Ag bond. This binding demonstrated that silver bound to titanium and reduced the band gap energy (Fig. 4). However, the amount of silver did not react completely but was oxidized under temperature to form Ag_2O. So, the XRD patterns showed the presence of Ag_2O. The free Ag_2O present in glass will also promise to improve the bactericidal ability of this material.

Conclusion

This study used the base glass composition of 73.8% Bi_2O_3 - 15.3% B_2O_3 - 10.9% ZnO (%w.t) to investigate the optical properties when adding TiO_2 or Ag/TiO_2. In the amorphous state on the XRD patterns, the bonds of $[BO_3]^{3-}$, $[BO_4]^{5-}$, $[BiO_3]^{3-}$, and $[BiO_6]^{9-}$ on the FTIR spectrum proved to be possible to make the BBZ at 1200°C for 90 minutes. When TiO_2 or Ag/TiO_2 were added to the matrix glass, the XRD and FTIR results of the samples also showed that TiO_2 and Ag not only participated in glass formation but also formed anatase, rutile and Ag_2O crystals distributed on the amorphous background. These crystals have increased reflectance and reduced transmittance of the base glass. Calculating the band gap of the glass systems from the UV-Vis spectrum has shown that the band gap energy of the background glass system is low (2.098 eV). The band gap energy increased with the addition of TiO_2 (2.478 eV of 5% TiO_2 and 2.695 eV of 10% TiO_2). The band gap energy decreased slightly with the addition of Ag/TiO_2 (2.336 eV of 1% Ag/5% TiO_2 and 2.642 eV of 1% Ag/10% TiO_2). The presence of anatase and rutile increased the band gap energy of the increased glass system. Thanks to the photocatalytic properties of anatase, rutile and the bactericidal ability of free Ag_2O, the BBZ combined with TiO_2 or Ag/TiO_2 can be applied as a low-temperature surface coating material antibacterial ability.

Acknowledgement

We acknowledge the support of time and facilities from Ho Chi Minh City University of Technology (HCMUT), VNU – HCM for this study.

References

1. G. Wei, F. Luo, B. Li, Y. Liu, J. Yang, Z. Zhang, Y. Liu, X. Shu, Y. Xie, and X. Lu, Ann. Nucl. Energy 150 (2021) 107817.
2. W. Yang, Q. Sun, Q. Lei, W. Zhu, Y. Li, J. Wei, and M. Li, J. Mater. Process. Techol. 267 (2019) 61-67.
3. J.H. Yi, Y.N. Ko, H.Y. Koo, D.S. Jung, and Y.C. Kang, J. Ceram. Process. Res. 12 (2011) 122-125.
4. J.Y. Song, T.J. Park, and S.Y. Choi, J. Non – Cryst. Solids 352 (2006) 5403-5407.
5. H. Zeng, Z. Liu, Q. Jiang, B. Li, C. Yang, Z. Shang, J. Ren, and G. Chen, J. Eur. Ceram. Soc. 34 (2014) 4383-4388.
6. S. Wiltzsch, Glass Technol-Part A 57 (2016) 15-19.
7. T. Luttrell, S. Halpegamage, J. Tao, A. Kramer, E. Sutter, and M. Batzill, Sci. Rep. 4 (2014) 1-8.
8. Y. Nosaka and A.Y. Nosaka, J. Phys. Chem. Lett. 7 (2016) 431-434.
9. C. Fredericci, H. Yoshimura, A. Molisani, and H. Fellegara, J. Non – Cryst. Solids 354 (2008) 4777-4785.
10. D. Ning, A. Zhang, M. Murtaza, and H. Wu, J. Alloys Compd. 777 (2019) 1245-1250.
11. L. Lu, G. Wang, Z. Xiong, Z. Hu, Y. Lioa, J. Wang, and J. Li, Ceram. Int. 46 (2020) 10667-10677.
12. R. Liu, P. Wang, X. Wang, H. Yu, and J. Yu, J. Phys. Chem. C 116 (2012) 17721-17728.
13. Q.L. Feng, J. Wu, G.Q. Chen, F.Z. Cui, T.N. Kim, and J.O. Kim, J. Biomed. Mater. Res. 52 (2000) 662-668.
14. Y.J. Kim, S.J. Hwang, and H.S. Kim, Mater. Sci. Forum 510-511 (206) 578-581.
15. Ö.B. Mergen and E. Arda, Synth. Met. 269 (2020) 116539.
16. P. Jitti-a-porn, S. Suwanboon, P. Amornpitoksuk, and O. Patarapaiboolchai, J. Ceram. Process. Res. 12 (2011) 85-89.
17. V. Anand, S. Sakthivelu, K.D.A. Kumar, S. Valanarasu, V. Ganesh, M. Shkir, S. Alfaify, and H. Algarni, J. Sol-Gel Sci. Techn. 86 (2018) 293-304.
18. Y.S. Song, M.H. Lee, B.Y. Kim, and D.Y. Lee, J. Ceram. Process. Res. 20 (2019) 182-186.
19. A. León, P. Reuquen, C. Garín, R. Segura, P. Vargas, P. Zapata, and P.A. Orihuela, Appl. Sci. 7 (2017) 49.
20. Y.H. Kim, M.Y. Yoon, E.J. Lee, and H.J. Hwang, J. Ceram. Process. Res. 13 (2012) 37-41.
21. M.A. Pandarinath, G. Upender, K.N. Rao, and D.S. Babu, J. Non – Cryst. Solids 433 (2016) 60-67.
22. D.H. Fan, R. Zhang, W.A. Su, and J.Z. Zhang, Mater. Sci. Technol. 31 (2014) 37-42.
23. A.A. Najim, Mater. Sci. Semicond. Process. 71 (2017) 378-381.
24. M.I. Sayyed, I.A. El-Mesady, A.S. Abouhaswa, A. Askin, and Y.S. Rammah, J. Mol. Struct. 1197 (2019) 656-665.
25. Q. Chen, Q. Wang, Q. Ma, and H. Wang, J. Non – Cryst. Solids 464 (2017) 14-22.
26. R.T. Tom, A.S. Nair, N. Singh, M. Aslam, C.L. Nagendra, R. Philip, K. Vijayamohanan, and T. Pradeep, Langmuir 19 (2003) 3439-3445.
27. M. Ali, J. Ceram. Process. Res. 15 (2014) 290-293.
28. H. Sutrisno and Sunarto, J. Ceram. Process. Res. 18 (2017) 378-384.
29. G. Liu, G. Wang, Z. Hu, Y. Su, and L. Zhao, Appl. Surf. Sci. 465 (2019) 902-910.